Dynamic Article Links ▶

PAPER

The immobilisation of chiral organocatalysts on magnetic nanoparticles: the support particle cannot always be considered inert†

Oliver Gleeson,[a] Gemma-Louise Davies,[b] Aldo Peschiulli,[a] Renata Tekoriute,[b] Yurii K. Gun'ko*[b] and Stephen J. Connon*[a]

A systematic study concerning the immobilisation onto magnetic nanoparticles of three useful classes of chiral organocatalyst which rely on a confluence of weak, easily perturbed van der Waals and hydrogen bonding interactions to promote enantioselective reactions has been undertaken for the first time. The catalysts were evaluated in three different synthetically useful reaction classes: the kinetic resolution of *sec*-alcohols, the conjugate addition of dimethyl malonate to a nitroolefin and the desymmetrisation of *meso* anhydrides. A chiral bifunctional 4-*N*,*N*-dialkylaminopyridine derivative could be readily immobilised; the resulting heterogeneous catalyst is highly active and is capable of promoting the kinetic resolution of *sec*-alcohols with synthetically useful selectivity under process-scale friendly conditions and has been demonstrated to be reusable in a minimum of 32 consecutive cycles. The immobilisation of a cinchona alkaloid-derived urea-substituted catalyst proved considerably less successful in terms of both catalyst stability and product levels of enantiomeric excess. An immobilised cinchona alkaloid-derived sulfonamide catalyst was also prepared, with mixed results: the catalyst exhibits outstanding recyclability on a par with that associated with the successful *N*,*N*-dialkylaminopyridine analogue, however product enantiomeric excess is consistently lower than that obtained using the corresponding homogeneous catalyst. While no physical deterioration of the heterogeneous catalysts was detected on analysis after multiple recycles, in the cases of both the conjugate addition to nitroolefins and the desymmetrisation of *meso* anhydrides, significant levels of background catalysis by the nanoparticles in the absence of the organocatalyst was detected, which explains in part the poor performance of the immobilised organocatalysts in these reactions from a stereoselectivity standpoint. It seems clear that the immobilisation of sensitive chiral organocatalysts onto magnetite nanoparticles does not always result in heterogeneous catalysts with acceptable activity and selectivity profiles, and that consequently the applicability of the strategy must be ascertained (until more data is available) on a case-by-case basis.

Introduction

In theory, a catalyst should emerge unaltered from a reaction it promotes, and therefore its perpetual use should be theoretically possible. In practice this is difficult, largely due to (partial) decomposition, product inhibition or mechanical loss on recovery. Therefore there has been considerable recent interest in the immobilisation of stable, largely moisture insensitive small molecule organocatalysts on heterogeneous supports, with the idea that

these stable materials can be separated from solution after reaction by filtration and subsequently reused.[1]

The main disadvantages associated with the immobilisation of organocatalysts on polymer supports include reduced reaction rates associated with mass transfer and (particularly in the case of polystyrene-based supports[2]) the requirement for a filtration step (inconvenient on process scale) and physical degradation of the support (particularly in the case of polystyrene-based supports- often with concomitant mechanical loss on filtration) upon continual reuse.

In an attempt to circumvent some of these difficulties, attention has recently begun to focus on the use of magnetic nanoparticles as heterogeneous organocatalyst supports.[3,4] The key premise underpinning the design of these catalysts is that a combination of a robust, high surface area support with moisture insensitive small molecule catalysts potentially allows the practitioner to aspire towards the design of catalysts of genuinely high recyclability.[5]

[a]Centre for Synthesis and Chemical Biology, School of Chemistry, Trinity College Dublin, Dublin, 2, Ireland. E-mail: connons@tcd.ie; Fax: +35316712826

[b]School of Chemistry and CRANN, Trinity College Dublin, Dublin, 2, Ireland. E-mail: igounko@tcd.ie; Fax: +35316712826

† Electronic supplementary information (ESI) available: Synthesis of all catalysts, general procedures, FTIR spectra, TGA curves, XRD patterns, NMR spectra and HPLC chromatograms. See DOI: 10.1039/c1ob06110k

This journal is © The Royal Society of Chemistry 2011

Org. Biomol. Chem., 2011, **9**, 7929–7940 | 7929

Another key advantage associated with such systems is that a filtration step is not required (which is particularly useful in process-scale applications)- the catalyst can be separated from the crude reaction mixture upon exposure to an external magnet and subsequent decantation.

In 2007, we developed the first 'hypernucleophilic' 4-*N*,*N*-dimethylaminopyridine (DMAP)[6] catalyst immobilised on magnetite nanoparticles. The resultant heterogeneous catalyst was highly active and recyclable in acyl transfer processes, Stieglitz rearrangements and hydroalkoxylation[7] reactions at loadings between 1 and 10% and could be recovered and recycled over 30 times without any discernible loss of activity.[8] Given the unprecedented recyclability exhibited by this catalyst, we were naturally eager to apply this immobilisation technology to more valuable, chiral catalyst systems. The literature is replete with examples of systems where highly active and selective chiral homogeneous organocatalyst systems have, on immobilisation, resulted in heterogeneous catalysts of moderate recyclability (*i.e.* <10 cycles) and diminished capability to promote highly enantioselective reactions.[1] Thus the identification of a high-surface area solid (magnetically recoverable) support which does not interfere in catalysis to any appreciable extent would represent a significant development in the field.

We therefore set out to answer two questions: firstly, can magnetite nanoparticles be used to generate chiral heterogeneous catalysts with activity and selectivity profiles not significantly different from that of their parent homogeneous analogues? Secondly, how broad is the potential scope of this strategy—can it be extended with advantage beyond DMAP-based systems to other proven organocatalysts which rely on weak interactions (particularly hydrogen bonding and general acids/base catalysis)?

We selected three classes of homogeneous organocatalyst systems for immobilisation: the chiral DMAP[9,10] derivative **1**, the bifunctional (thio)urea-substituted cinchona alkaloid catalysts **2**–**3** and the analogous sulfonamide system **4**. Catalyst **1**- which is readily accessible from L-proline- has been demonstrated to be capable of promoting highly enantioselective acylation reactions.[11] It has also found application in the development of a chemically driven information ratchet.[12] The second (thio)urea system (*i.e.* **2**–**3**, Fig. 1) has been the focus of intensive investigation over the past six years[13] -for example our group (among others) have shown that these catalysts promote enantioselective Michael addition-,[14] Dynamic Kinetic Resolution- (DKR),[15] desymmetrisation-,[16] Henry reaction-[17] and transthioesterification[18] processes, while others have demonstrated their utility in a range of applications-mostly in either addition or cycloadditions reactions.[19] The third sulfonamide-based catalyst system (*i.e.* **4**) has emerged recently.[20]
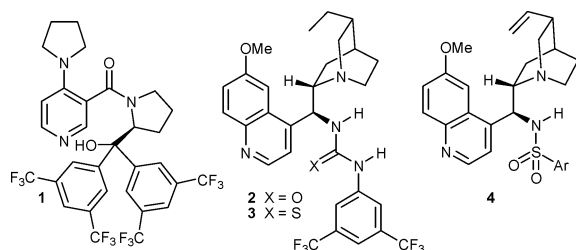
This class of catalyst has been shown to promote highly efficient desymmetrisations of *meso*-anhydrides by alcoholysis[21] and has also been utilised in a tandem desymmetrisation/thiol kinetic resolution reaction.[22] The three catalyst systems are readily prepared, they are air/moisture insensitive and they represent a reasonably broad (in an organocatalytic context) range of characteristics (pK_a, basicity/nucleophilicity, reaction mechanism and substrate scope *etc.*), the interaction (if any) of which with magnetite nanoparticle supports would be interesting to determine.

In a preliminary communication,[23] we detailed the design and evaluation of catalyst **5**- an immobilised variant of **1**- as a recyclable promoter of the acylative KR of *sec*-alcohols. This strategy was gratifyingly simple to implement- the catalyst could be readily prepared (the magnetite nanoparticles of 7.9 ± 1.5 nm were prepared *via* the coprecipitation technique),[24,25] the loading could be monitored by ^{1}H NMR spectroscopy, and the activity/selectivity profiles were excellent: for example, the racemic alcohol **6** could be asymmetrically acylated at ambient temperature in the presence of a relatively low loading of catalyst (5 mol%) for 20 consecutive recycles (Scheme 1). The protocol was set up to be as practical and operationally simple as possible- *we utilised the cheap, unhindered acetic anhydride as the acylating agent at ambient temperature* (often artificial acylating agents require the use of low reaction temperatures and more hindered and expensive anhydrides such as (*i*BuCO)$_2$O to obtain high selectivity).[10,11,26] After each reaction, the catalyst was easily separated from the products by exposure of the reaction vessel to an external magnet, followed by decantation of the reaction solution. The catalyst (which remains in the flask) was washed with THF to remove residual product and dried under high vacuum, whereupon it was ready for reuse. We have found that no special handling precautions regarding exposure to air/moisture need be taken in the use of catalyst **5**.
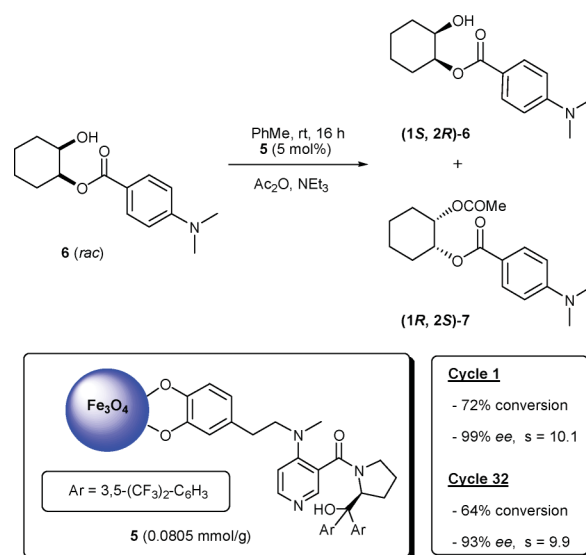
Scheme 1 Heterogeneous catalyst **5** as a promoter of acylative KR.

The same batch of catalyst **5** was then employed in the KR of other *sec*-alcohols and after having been used in 31 consecutive cycles, we returned the KR of **6** at ambient temperature. *We were delighted to find that the by now heavily recycled catalyst performed*

Fig. 1 Homogeneous bifunctional catalyst targets for immobilisation on magnetite nanoparticles.

exceptionally well, *promoting the acylation with a selectivity factor of 9.9* (*recovered alcohol −93% ee at 64% conversion*). In addition, TEM analysis of the nanoparticles after the 32nd cycle indicated a complete absence of particle degradation.

The immobilisation of the chiral DMAP-derivative exceeded our expectations: it has been shown that a chiral organocatalyst which relies on a confluence of weak, easily perturbed van der Waals and hydrogen bonding interactions to promote enantioselective reactions can be readily immobilised on magnetite nanoparticles and that the resulting heterogeneous catalyst is highly active and is capable of promoting the kinetic resolution of *sec*-alcohols with synthetically useful selectivity under process-scale friendly conditions (ambient temperature, low catalyst loading and acetic anhydride as the acylating agent)- which allows the isolation of resolved alcohols with good-excellent enantiomeric excess. Perhaps most importantly, the somewhat surprising lack of interaction between the nanoparticle core and the organocatalyst unit results in a chiral heterogeneous catalyst which is recyclable to an unprecedented extent- in this study it has been demonstrated to be reusable in a minimum of 32 consecutive cycles while retaining high activity and selectivity profiles. It is worthwhile to note that the previous literature benchmark for this class of supported chiral acylation catalyst was a Merrifield resin-supported system which could promote the KR of selected mono-protected *cis*-diols with good selectivity (S up to 13 but inconsistent between runs) and could be recycled four times.[26]

Results and discussion

Immobilisation of chiral bifunctional (thio)urea derivatives

We were next interested in an investigation of the effect of immobilisation on (thio)urea-based catalyst systems. These catalysts are of considerably broader scope (*vide supra*) than DMAP derivatives and would thus represent an attractive target for immobilisation. The interplay between the Brønsted-acidic and Brønsted-basic catalyst components of the homogeneous promoters **2** and **3** represents a more delicate balance than that associated with the corresponding DMAP-based catalyst **1**, and as such any interaction between the catalyst and the solid support would be likely to disrupt the activity/selectivity profile considerably. The sparse literature concerning the immobilisation of bifunctional (thio)urea catalysts is not yet extensive enough to allow conclusions to be drawn on the suitability of these catalysts for immobilisation: for instance one report concerning their immobilisation on mesoporous silica surfaces indicates that improved activity/selectivity can be achieved relative to the homogeneous system,[27] while another clearly indicates that considerably reduced activity results on loading a bifunctional[28] thiourea catalyst onto either polystyrene or polyethylene glycol.[29] In both cases continuous recyclability was poor (<6 cycles).

To determine if magnetite could serve as a useful support for these catalysts we synthesised the immobilised bifunctional urea **8** as follows: addition of the thiol **10** to the known quinine-derived urea **9** in the presence of AIBN afforded the sulfide **11**,[30] which could be isolated and then loaded onto magnetite nanoparticles as before (using 4-iodoanisole as an internal standard to facilitate quantitative ^{1}H NMR spectroscopic analysis) with 100% efficiency to afford **8** with a catalyst loading of 0.1 mmol g^{-1} (Scheme 2).
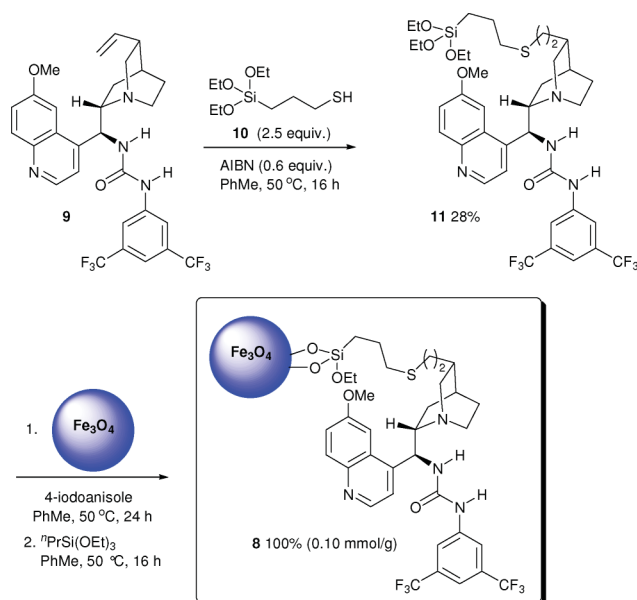
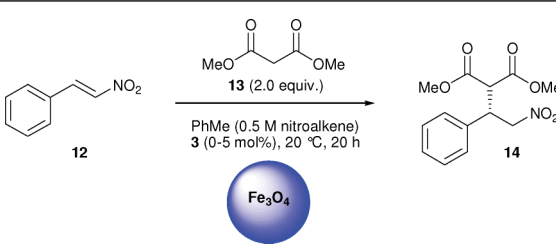**Scheme 2** Synthesis of the immobilised bifunctional urea **8**.

Attempted clean synthesis of the corresponding thiourea analogue repeatedly produced complex mixtures involving catalyst decomposition and incomplete loading, in addition the resulting heterogeneous catalyst failed to perform reproducibly in a range of processes known to be susceptible to the influence of the homogeneous catalyst **3**.

Catalyst **8** however, exhibited no such instability initially. This catalyst was evaluated as a promoter of the asymmetric addition of dimethyl malonate (**13**) to (*E*)-β-nitrostyrene (**12**). We had previously reported[14a] that this reaction could be catalysed by **2** (at 5 mol% loading) to furnish adduct **14** in 74% *ee* in 5 h reaction time.[31] Under identical conditions use of the immobilised material **8** allowed the formation of **14** in a comparable 71% *ee* (Table 1, entry 1), however the catalyst's activity proved disappointing: only 70% conversion of **12** was recorded after 24 h. While the catalyst initially appeared to be as robust as the heterogeneous DMAP-derivative **5** (product enantiomeric excess actually increased during cycles 2 and 3, entries 2–3: we note that this 'ageing' effect was previously observed by Takemoto in the use of a homogeneous PEG-immobilised thiourea-based catalyst),[29]

Table 1 Immobilised urea **8**: Asymmetric catalysis of a Michael addition reaction

Entry	Cycle	Conversion (%)^a	ee (%)^b
1	1	70	71
2	2	70	72
3	3	71	77
4	4	46	n.d.

^{a} Conversion determined by ^{1}H NMR spectroscopy. ^{b} Determined by CSP-HPLC.

**Table 2** Investigation of the potential influence of the nanoparticles on product enantiomeric excess

Entry	Catalyst Loading (mol%)	Nanoparticle Loading (mg mg^{-1} of **12**)	Conv. (%)[a]	ee (%)[b]
1	0	0	0	—
2	5	0	90	94
3	0	3.36	6	0
4	5	3.36	100	84

[a] Conversion determined by ^{1}H NMR spectroscopy. [b] Determined by CSP-HPLC.

it ultimately proved incapable of promoting the reaction with appreciable efficacy after 4 cycles (entry 4). This instability was unfortunately a characteristic of each catalyst batch prepared and points to an inherent design limitation rather than any kind of mishandling during experimentation. It is also interesting to note that we found that the decline in catalyst performance was more a function of time elapsed since loading rather than the number of iterative recycles the catalyst had been used in.

We next carried out three experiments aimed at investigating the potential role (if any) of the nanoparticle in reducing the catalyst efficacy from a stereoselectivity perspective (Table 2). As expected, we observed no background uncatalysed reaction between **12** and **13** in the absence of either catalyst or nanoparticle (entry 1). The homogeneous catalyst **3**— in the absence of nanoparticles, promoted the reaction with excellent enantioselectivity (entry 2). It is important to note that these reactions were carried out using a mechanical shaker, to ensure that the experimental conditions are as close as possible to those associated with the use of the heterogeneous catalyst **8**. We were surprised to find that the nanoparticles themselves (when utilised in identical mass loadings to that used in the application of the heterogeneous catalyst **8**) catalysed the formation of (*rac*)-**14** in the absence of **3** (entry 3). This is disappointing— as in the acylation study (*vide supra*) the nanoparticles themselves were completely inert— however it explains (at least in part) the origin of the relatively poor levels of product *ee* observed in reactions catalysed by **8**. To confirm this hypothesis, we repeated the conjugate addition in the presence of both **3** and the nanoparticles: as expected **14** was isolated with only 84% *ee* (entry 4), which indicates that the nanoparticles (despite attempts to protect the surface through siloxane functionalisation) compete with **3** for the substrate to an appreciable extent under these conditions.

In an attempt to better understand the fate of catalyst **8** after multiple cycles, we characterised three batches of nanoparticles: one batch which had not been loaded with catalyst, one which had been loaded but then simply stored under argon and not used in any catalytic processes, and finally the batch associated with the data outlined in Table 1.
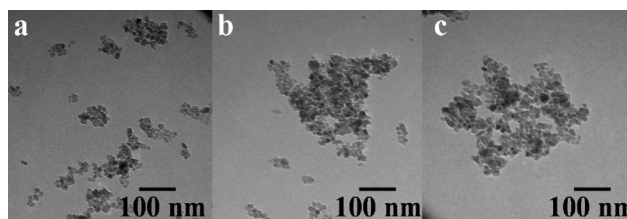

Fig. 2 TEM images of (a) magnetite nanoparticles, (b) urea catalyst-loaded nanoparticles (**8**) and (c) urea catalyst-loaded nanoparticles (**8**) after recycling several times. Scale bar 100 nm.

According to TEM analysis, the average particle diameter was 10 ± 2 nm (Fig. 2). After loading the nanoparticles with catalyst to prepare **8** and after recycling several times, the TEM images show no changes in either nanoparticle size or morphology, however they do appear slightly more aggregated.

FTIR analysis showed that the catalyst had been successfully functionalised onto the magnetite nanoparticles (ESI†).[24] It also demonstrated that no degradation or damage appeared to occur as a result of recycled use. Interestingly, TGA analysis indicated that the amount of organic material on the catalyst-loaded nanoparticles appeared to increase after recycling, indicating a minute alteration in the compound due to multiple uses (ESI†). This change could be responsible for the decrease in the catalytic activity over time. The nature of the change however is not obvious, as FTIR and XRD analysis (ESI†) displayed no changes in the composition of the core nanoparticles or the nature of the organic functionalities.

Immobilisation of chiral bifunctional sulfonamide derivatives

Given the somewhat surprising lack of recyclability of the urea-based catalyst **8** (*vide supra*), our attention turned to the immobilisation of the sulfonamide derivatives of general type **4**. Song has shown that a polystyrene-supported sulfonamide-based catalyst **15** (Fig. 3) could promote the methanolytic desymmetrisation of *meso* succinic-anhydrides with >90% *ee* and 3-phenyl glutaric anhydride with 89% *ee*. Remarkably for a polystyrene-based material, the catalyst proved extremely recyclable and could be used 10 times without loss of either activity or selectivity.[32] This undoubtedly represents the literature benchmark in heterogeneous catalysis of this asymmetric process.[33]
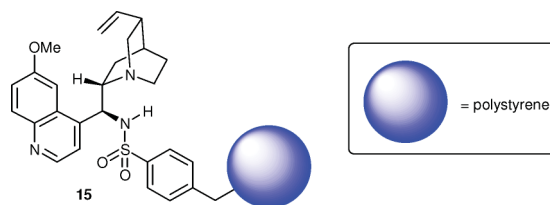
Fig. 3 A polystyrene-supported organocatalyst reported by Song *et al.*

The asymmetric addition of alcohols to *meso* anhydrides is a reaction we have had considerable interest in from a homogeneous catalysis perspective,[16,22] and we were thus intrigued as to the potential of a nanoparticle-immobilised sulfonamide-based catalyst, where we envisaged that the lower Lewis-basicity and considerably augmented hydrolytic stability characteristics of the

Table 3 Selection of the optimal aryl sulfonamide group in a homogeneous model system

Entry	Catalyst	Time (h)	ee (%)[a]
1	**4b**	20	87
2	**4c**	20	85
3	**4d**	20	82
4	**4e**	52	75

[a] Determined by CSP-HPLC.

Table 4 Evaluation of the homogeneous catalyst **4b** in the desymmetrisation of *meso* succinic anhydrides

Entry	Substrate	Product	Time (h)	Conv. (%)[a]	ee (%)[b]
1	**18**	**21**	6	87	95
2	**19**	**22**	6	85	94.5
3[b]	**20**	**23**	18	99[c]	96.5

[a] Conversion determined by ^{1}H NMR spectroscopy. [b] Reaction at 0.05 M concentration. [c] Isolated yield.

sulfonamide functional group relative to the urea would prove a distinct advantage in terms of catalyst recyclability.

The design process began with the selection of the sulphonamide aryl group. To facilitate the rapid evaluation of catalysts incorporating several different aryl moieties in this particular reaction the homogeneous model sulfonamides **4b–4e** were prepared and compared in the desymmetrisation of *meso* anhydrides by methanolysis (Table 3).[34] Before discussing the data, two points are noteworthy: firstly, since we intended to eventually investigate the use of nanoparticle-supported catalysts, we decided to only evaluate the homogeneous model systems under conditions likely to be both operationally convenient and conducive to smooth heterogeneous catalysts later on, thus reactions were carried out using the traditionally challenging 3-methyl glutaric anhydride (**16**) substrate (so that the potential limits of the catalyst could be identified early), and both low temperature and high dilution conditions (known to be beneficial to enantioselectivity in these reactions but likely to be a problem when used in conjunction with heterogeneous catalysis) were avoided. Secondly, we had experience of the use of these materials in a related process involving simultaneous kinetic resolution and *meso* anhydride desymmetrisation,[22] and from these studies had divined that **4b** was a more efficacious promoter of the desymmetrisation of glutaric anhydrides in that process than the literature catalyst **4a**,[21] therefore the latter catalyst was excluded from this study.

The results of these initial experiments are outlined in Table 3. The pentafluoro-substituted catalyst **4b** (entry 1) represented a useful combination of superior activity and ability to promote the reaction (at low loading, ambient temperature and 0.1 M concentration) with higher levels of product *ee* than either the less acidic **4c** (entry 2) or the more hindered (and also less acidic) **4d** and **4e** (entries 3 and 4) and was therefore selected for further investigation.

To ensure that **4b** was compatible with other synthetically relevant substrates, it was then utilised in the desymmetrisation of a selection of succinic *meso* anhydrides under identical conditions (Table 4).

The catalyst performance here was most satisfactory. Anhydrides **18–20** could be converted to either acyclic or cyclic hemiesters **21** (entry 1) and **22–23** (entries 2–3) respectively in excellent enantiomeric excess at ambient temperature using a catalyst loading of 2 mol%.

Encouraged by the excellent catalytic abilities exhibited by sulfonamide **4b** under homogeneous conditions, we decided to synthesise a nanoparticle-supported heterogeneous analogue and concentrated our attention on the identification of a suitable immobilisation strategy. Again we chose the quinuclidine vinyl group, which is not located in close proximity to the catalytically relevant functionality (*i.e.* the acidic sulfonamide proton and the quinuclidine nitrogen), as the location at which to anchor the nanoparticle *via* a sulfide tether. After some experimentation, reproducible conditions for the synthesis of the supported catalyst **37** were identified (Scheme 3): treatment of sulfonamide **4b** with excess **10** in toluene at 60 °C and in the presence of AIBN (50 mol%), led to the isolation of **25** in 65% yield after purification by flash-chromatography. The subsequent loading step involving this new species could then be conveniently accomplished by allowing **25** to react with magnetite nanoparticles (average particle size 9.7 ± 3.5 nm), in CDCl$_3$ at 50 °C under mechanical agitation, in the presence of 2,5-diphenylfuran as an internal standard (Scheme 3). The catalyst loading (1.00 mmol g^{-1}) was determined as before by ^{1}H NMR spectroscopic analysis of a sample of the reaction mixture after 20 h. No traces of the resonances corresponding to either **25** or derived decomposition products were detected. Capping of the particles with *n*-propyl triethoxysilane was not carried out as no advantage in terms of catalyst performance was observed in catalyst batches which had been treated with this reagent.

As before, both the nanoparticle batch utilised in the loading process and the loaded catalyst itself were characterised.
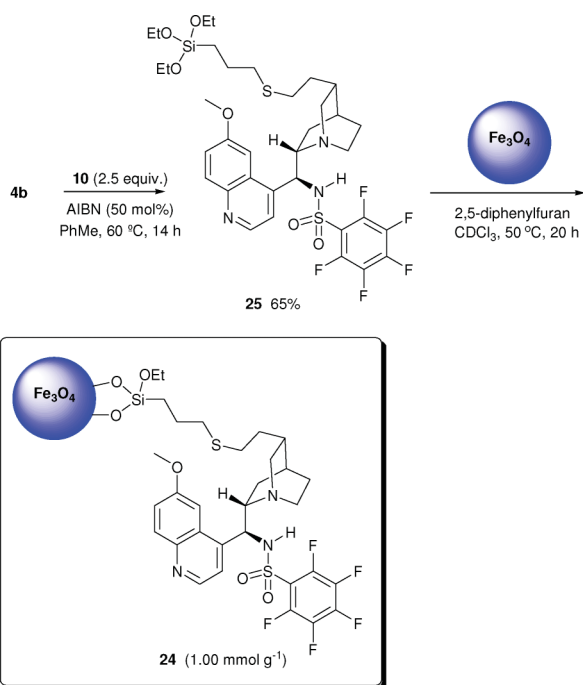
Scheme 3 Synthesis of the immobilised bifunctional sulfonamide **24**.

Table 5 Evaluation of **24** as a recyclable catalyst in the desymmetrisation of **20**

Entry	Cycle	Conversion (%)[a]	ee (%)[b]
1	1	100	80
2	2	99	80
3	3	99	80
4	4	98	78
5	5	98	78
6	6	98	78
7	7	99	77
8	8	97	77
9	9	98	77
10	10	97	78
11	11	97	77
12	12	97	77
13	13	96	77
14	14	97	77
15	15	96	78
16	16	96	77
17	17	96	77
18	18	97	77
19	19	96	77
20	20	97	77

[a] Determined by ^{1}H NMR spectroscopy. [b] Determined with excellent agreement by either CSP-HPLC or ^{1}H NMR spectroscopic analysis after derivatisation, see Experimental Section.

According to TEM analysis, the average nanoparticle size was 9.7 ± 3.5 nm. After loading the nanoparticles with catalyst, the TEM images show no changes in either the size or behaviour of the nanoparticle (Fig. 4).
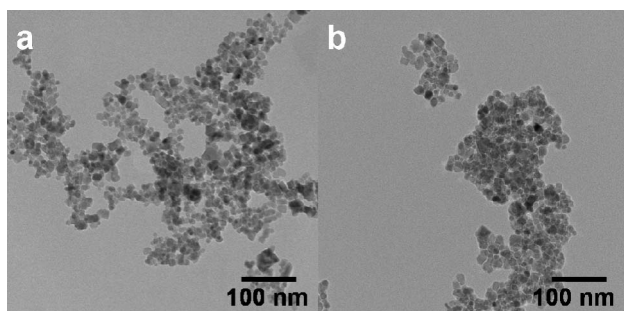

Fig. 4 TEM images of (a) magnetite nanoparticles and (b) catalyst loaded nanoparticles (**24**). Scale bar 100 nm.

FTIR spectroscopy and TGA analysis of the samples confirmed that the sulfonamide catalyst had been successfully loaded onto the surface of the nanoparticles (ESI†).[24] XRD also confirms no changes or degradation of the magnetite core occur (ESI†).[24]

Catalyst **24** was then evaluated as a recyclable promoter of the asymmetric ring-opening of **20** (Table 5). We found **24** to be highly recyclable— it could be reused in twenty consecutive cycles without any significant decrease in catalytic activity and enantioselectivity. We observed near quantitative conversion of **20** to product **23** after 18 h in the first three cycles of our recyclability study (entries 1–3) and only a slight decrease in catalyst activity between cycles 3 and 20: for instance conversion in cycle 20 was determined to be 97% (entry 20)— which is strongly indicative that **24** is not decomposing significantly between runs. From a chiral information transfer standpoint the catalyst is also robust: only a

very small diminution of product *ee* was observed between the first and 20th iteration, with all reactions being carried out at ambient temperature. However the magnitude of asymmetric induction— which lay in the range of 80% (cycles 1–3, entries 1–3) to 77% (*e.g.* cycle 20, entry 20)— was disappointing relative to that associated with the use of the homogeneous analogue **4b** (Table 3).

The same catalyst batch utilised in the experiments outlined in Table 5 was then tested in the desymmetrisation of a set of monocyclic, bicyclic and tricyclic prochiral anhydrides (Table 6). Thus, when bicyclic-succinic anhydride **19** was treated with MeOH (10 equiv.) in the presence of 5 mol% of **24**, the corresponding hemiester could be isolated in 97% yield and 78% *ee* after 24 h (cycle 21, entry 1). The consistency of such findings was confirmed by repeating the desymmetrisation of **19** under identical conditions in two subsequent consecutive cycles (78–79% *ee*, cycles 22–23, entries 2–3). Reproducible results were also observed in the methanolysis reaction of **18** (cycles 24–26, entries 4–6) that yielded hemiester **22** in 78% *ee* (average value from three consecutive runs). The desymmetrisation protocol was found to be compatible with more challenging, sterically demanding substrates, such as tricyclic anhydrides **26** and **27**: the *endo*-hemiester **28** was isolated in 92% yield and 82% *ee* (cycle 27, entry 7) after 4 d at room temperature, while in the case of the formation of the corresponding *exo*-adduct (*i.e.* **29**) we observed a slightly lower level of product enantiopurity (79% *ee*, cycle 28, entry 8).

We had previously found that methanol could be advantageously replaced with allyl alcohol in the desymmetrisation reaction of succinic anhydrides.[15] This is useful as we previously demonstrated that the adduct in these cases could be readily converted to the enantiomer of that which one obtains from

7934 | *Org. Biomol. Chem.*, 2011, **9**, 7929–7940

This journal is © The Royal Society of Chemistry 2011

Table 6 Evaluation of **24** in the desymmetrisation of *meso* succinic anhydrides

Entry	Cycle	Substrate	Product	Yield (%)[a]	Ee (%)[b]
1	21	**19**	**22**	97	78
2	22			96	78
3	23			96	79
4	24	**18**	**21**	94	78
5	25			92	77
6	26			94	78
7[c]	27	**26**	**28**	92	82
8[c]	28	**27**	**29**	97	79

[a] Isolated Yield. [b] Determined by ^{1}H NMR spectroscopic analysis after derivatisation, see Experimental Section. [c] 10 mol% of catalyst used, 96 h reaction time.

direct methanolysis of the substrate with the *other antipode of the catalyst* (*i.e.* enantiodivergent synthesis) after a simple esterification/deprotection sequence.[15] In cycle 29 we therefore investigated the desymmetrisation reaction of anhydride **20** with allyl alcohol in the presence of catalyst **24**. We were pleased to find that hemiester **30** was obtained with enhanced enantiopurity (82% *ee*) and in 83% yield after 48 h (Scheme 4).
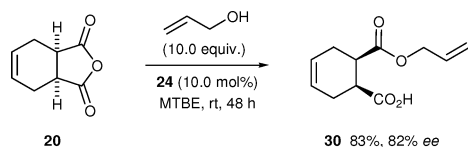

Scheme 4 Cycle 29: Desymmetrisation using allyl alcohol as the nucleophile.

Finally, to further investigate the robust nature of **24**, we returned to the desymmetrisation reaction of anhydride **20** under identical conditions to those used in the first iterative cycle involving this catalyst (*i.e.* Table 5, entry 1). Gratifyingly, we found that, after being used for 29 consecutive runs, **24** could still perform exceptionally well, promoting the formation of hemiester **23** to a satisfying level of conversion (95%, 92% isolated yield) and in 78% *ee* (Scheme 5). If one compares this to the data obtained
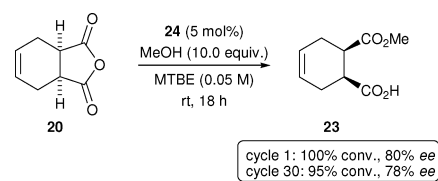
Scheme 5 Cycle 30: A repeat of the first iterative cycle to examine catalyst loss/decomposition.

in the first cycle (shown in Scheme 5), the outstanding durability of sulfonamide **24** is readily apparent: after 30 cycles the catalyst retains almost all of its activity and ability to discriminate the two prochiral carbonyl substrate moieties: the reduction in catalyst performance through either mechanical loss or decomposition over 30 iterative recycles is perceptible, but minimal.

Finally, we carried out a pair of control experiments as before to investigate the potential of the nanoparticle support to act as a catalyst in this process (at the same mass loadings as used in Tables 5 and 6). We found that both batches of nanoparticles which had been capped with *n*-PrSi(OEt)₃ and those which had not been treated were capable of serving as catalysts in the alcoholysis of **19** (Scheme 6). In the case of the uncapped particles, catalysis was extraordinarily effective, while even the capped material proved efficient enough a promoter of the formation of (*rac*)-**22** for it to be considered a credible cause of the reduced levels of enantiomeric excess observed using **24** relative to its homogeneous analogue **4b**.
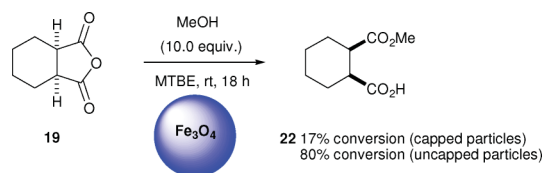
Scheme 6 Background catalysis of anhydride alcoholysis by magnetic nanoparticles.

Conclusions

A systematic study concerning the immobilisation onto magnetic nanoparticles of three useful classes of chiral organocatalyst which rely on a confluence of weak, easily perturbed van der Waals and hydrogen bonding interactions to promote enantioselective reactions has been undertaken for the first time. The catalysts were evaluated in three different synthetically useful reaction classes: the kinetic resolution of *sec*-alcohols, the conjugate addition of dimethyl malonate to a nitroolefin and the desymmetrisation of *meso* anhydrides. Somewhat surprisingly, it is clear that, despite early indications to the contrary, the success of this strategy hinges on the structure of the catalyst being immobilised. In the case of chiral DMAP derivatives such as **1** (*i.e.* catalyst **5**) the resulting heterogeneous catalyst is highly active and is capable of promoting the kinetic resolution of *sec*-alcohols with synthetically useful selectivity under process-scale friendly conditions (ambient temperature, low catalyst loading and acetic anhydride as the acylating agent)- which allows the isolation of resolved alcohols with good-excellent enantiomeric excess. The magnetic catalyst is simple to prepare, insensitive to air/moisture and easily recoverable by exposure of the reaction vessel to an

external magnetic field. Perhaps most importantly, the lack of interaction between the nanoparticle core and the organocatalyst unit results in a chiral heterogeneous catalyst *which is recyclable to an unprecedented* extent— in this study it has been demonstrated to be reusable in a minimum of 32 consecutive cycles while retaining high activity and selectivity profiles.[35]

In stark contrast, urea catalyst **2** was demonstrated to be wholly incompatible with immobilisation onto magnetite nanoparticles. A marked drop in catalyst efficacy (from both activity and selectivity standpoints) is observed on immobilisation and the catalyst proved unstable over only a handful of iterative recycles. Most significantly, a short study aimed at uncovering the origin of this poor performance from a stereoselectivity perspective determined categorically that background catalysis by the particles themselves is problematic in the conjugate addition reaction under study. *This is a somewhat startling observation which should serve as a warning that these particles cannot be automatically considered to be inert in catalytic processes.*

The heterogeneous sulfonamide catalyst **24** represents an intermediate scenario: the catalyst exhibits outstanding recyclability on a par with that associated with the nucleophilic catalyst **5**, however product enantiomeric excess using the immobilised catalyst is consistently lower (*ca.* 80% *ee*) than that obtained using the corresponding homogeneous catalyst **4b**. Again, unhelpful background catalysis by the nanoparticle support was shown to be a likely cause of this phenomenon.

The compatibility of this magnetite nanoparticle immobilisation methodology with a dialkylaminopyridine organocatalyst known to be highly sensitive to its environment[11] is extremely promising. In particular, this emerging nanotechnology possesses strong potential for further general applicability at the frontiers of (asymmetric) catalysis. This study aims to highlight that carrier nanoparticles can and do interact with both the loaded catalyst, and (on occasion) the substrate- compromising either activity/stability or selectivity (or both). Therefore, it cannot be regarded as a general, all-encompassing solution to the problem of the design of genuinely recyclable, highly active and selective immobilised chiral organocatalysts. As such, studies are currently underway in our laboratory aimed at further charting the limits of this strategy on a case by case basis.

Experimental

General

Proton Nuclear Magnetic Resonance spectra were recorded on 400 and 600 MHz spectrometers in $CDCl_3$ referenced relative to residual $CHCl_3$ (δ = 7.26 ppm) and DMSO-d_6 referenced relative to residual DMSO (H) (δ = 2.51 ppm). Chemical shifts are reported in ppm and coupling constants in Hertz. Carbon NMR spectra were recorded on the same instruments (100 MHz and 150 MHz) with total proton decoupling. All melting points are uncorrected. Infrared spectra were obtained using neat samples on a diamond Perkin Elmer Spectrum 100 FT-IR spectrometer using a universal ATR sampling accessory. Flash chromatography was carried out using silica gel, particle size 0.04–0.063 mm. TLC analysis was performed on precoated 60F$_{254}$ slides, and visualised by either UV irradiation or $KMnO_4$ staining. Optical rotation measurements were made on a Rudolph Research Analytical

Autopol IV instrument and are quoted in units of 10^{-1} deg cm^2 g^{-1}. Toluene, ether and THF were distilled from sodium. Methylene chloride and triethylamine were distilled from calcium hydride. Ammonium hydroxide (NH_4OH, 0.88 M) was obtained from BDH Chemicals. Ferric chloride hexahydrate ($FeCl_3 \cdot 6H_2O$) and ferrous chloride tetrahydrate ($FeCl_2 \cdot 4H_2O$), were obtained as powders from Sigma-Aldrich. Acetic anhydride was freshly distilled before use. Analytical CSP-HPLC was performed on Daicel CHIRALCEL OD-H (4.6 mm × 25 cm), CHIRALPAK AD-H (4.6 mm × 25 cm) and AS (4.6 mm × 25 cm) columns. TEM images were obtained on a Jeol JEM-2100, 200 kV LaB$_6$ instrument, operated at 120 kV with a beam current of about 65 mA. Samples for TEM were prepared by deposition and drying of a drop of the powder dispersed in water onto a formvar-coated 300-mesh copper grid. Diameters were measured using the ImageJ version 1.40 software program; average values were calculated by counting a minimum of 100 particles. Samples for TEM were prepared by deposition and drying of a drop of the powder dispersed in Millipore water onto a formvar coated 400 mesh copper grid. The thermogravimetric analysis (TGA) was carried out on a Pyris 1 TGA from Perkin Elmer and the samples (1.5–2 mg) were burned in air at a constant heating rate of 10 °C min^{-1} from 30 to 900 °C. X-Ray powder diffraction was performed using a Siemens-500 X-Ray diffractometer. Powder samples were deposited on silica glass using silica gel to adhere the sample to the glass surface. Overnight spectra were run for all samples. Diffractograms were then compared to the JCPDS database. Unless otherwise stated, all other chemicals were obtained from commercial sources and used as received. Unless otherwise specified, all reactions were carried out in oven-dried glassware under an atmosphere of argon.

Synthesis of magnetite nanoparticles

Magnetite nanoparticles were prepared by the co-precipitation of $FeCl_2 \cdot 4H_2O$ and $FeCl_3 \cdot 6H_2O$ in a molar ratio of 1:2 with 0.5 M NaOH. This alkaline solution was stirred at 80 °C for 1 h, yielding a black colloidal suspension of magnetite nanoparticles which were washed several times with water until pH neutral. The nanoparticles were then dried under vacuum for 24 h.

Siloxane 11

A 5 mL round bottom flask, equipped with a stirring bar, was charged with urea **9** (300 mg, 0.52 mmol) and azobisisobutyronitrile (AIBN, 51 mg, 0.31 mmol). The flask was fitted with a septum and flushed with argon. Dry toluene (2.0 mL) was added *via* syringe followed by 3-mercaptopropyltriethoxysilane (**10**, 313 µL, 1.30 mmol) and the resulting mixture was heated to 60 °C and stirred for 16 h. The solvent was removed *in vacuo* and the residue purified by column chromatography (EtOAc-NEt$_3$ 90 : 10) to give **11** in 9.5% yield (40 mg) as an amorphous beige solid. Mp 77–81 °C; [α]$_D^{20}$ = +9.2 (*c* 1.0, CHCl$_3$); δ_H (400 MHz, CDCl$_3$) 0.72–0.76 (m, 2H), 0.97–1.02 (m, 1H), 1.21–1.25 (t, 9H), 1.47–1.76 (m, 9H), 2.10–2.19 (m, 1H), 2.33–2.39 (m, 2H), 2.49–2.53 (t, 2H), 2.70–2.77 (m, 1H), 3.06–3.17 (m, 2H), 1.09 (bs, 1H), 3.80–3.85 (q, 6H), 4.03 (s, 3H), 5.51 (bs, 1H), 6.19 (br s, 1H), 7.39–7.41 (m, 2H), 7.44–7.47 (dd, J 2.4, 6.8, 1H), 7.72–7.74 (m, 3H), 8.08–8.10 (d, J 9.2, 1H), 8.24 (br s, 1H), 8.85–8.86 (d, J 4.4, 1H); δ_C (100 MHz, CDCl$_3$) 9.9, 18.3, 23.2, 25.1, 26.9, 27.9, 29.7, 33.7, 34.4, 35.3, 41.5, 50.7,

55.8, 57.0, 58.4, 59.7, 101.9, 115.4, 188.0, 118.2 (q, $J_{19F-13C}$ 4 Hz), 122.5, 123.0 (q, $J_{19F-13C}$ 273 Hz) 128.5, 132.0, 132.0 (q, $J_{19F-13C}$ 30 Hz), 140.5, 144.3, 145.1, 147.2, 154.6, 158.5; δ_F (376 MHz, CDCl$_3$) −63.67; v_{max}(neat)/cm^{-1} 2974, 2928, 1703, 1622, 1566, 1509, 1387, 1276, 1241, 1226, 1169, 1101, 944, 780, 681; m/z (ES) 817.3267 (M + H$^+$. C$_{38}$H$_{50}$N$_4$O$_5$F$_6$SSi requires 816.3175).

Magnetic nanoparticle-supported urea catalyst 8

A 50 mL reaction vessel was charged with siloxane 11 (0.020 mmol, 16.3 mg) and 4-iodoanisole (internal standard, 0.0203 mmol, 4.7 mg). The reaction vessel was placed under an argon atmosphere and fitted with a septum and dry C$_6$D$_5$CD$_3$ (4.0 mL) was added via syringe. At this point ^{1}H NMR spectroscopic analysis ($t = 0$ min) was carried out. Magnetite nanoparticles (200.0 mg) were then added in one portion and the resulting suspension was sonicated for 5 min at room temperature. The resulting mixture was heated to 50 °C for 24 h under mechanical agitation. The vessel was then placed in proximity of an external magnet and the solution was separated from the nanoparticles via a Pasteur pipette. Catalyst loading (1.00 mmol g^{-1}) was determined by ^{1}H NMR spectroscopic analysis of the resulting solution which showed no traces of the peaks corresponding to the catalyst loading precursor. The remaining particles were subjected to five consecutive washing cycles with dry toluene (4.0 mL) which was decanted in the presence of an external magnet. In order to cap the remaining oxide surface of the nanoparticles, 5 mL of dry toluene was added to the nanoparticles under an Ar atmosphere, n-propyltriethoxysilane (1 mL) via syringe and the suspension shaken under mechanical agitation at 50 °C for 16 h. The reaction solution was decanted in the presence of an external magnet and the nanoparticles were washed five times with dry toluene (5 mL) before being evaluated as a recyclable catalyst.

General procedure for the addition of dimethyl malonate to (E)-β-nitrostyrene catalysed by 8

A 50 mL reaction vessel containing 8 (200 mg, 0.020 mmol) was charged with (E)-β-nitrostyrene 12 (59.6 mg, 0.400 mmol) and placed under an atmosphere of Ar (balloon). Dry toluene (6 mL) was added via syringe and the resulting suspension shaken under mechanical agitation for ca. 30 min. Dimethyl malonate 13 (91 µL, 0.800 mmol) was then added via syringe and the suspension shaken for a further 20 h at room temperature. The reaction was stopped by placing the reaction vessel over an external magnet. The reaction vessel was kept over the external magnet until the reaction suspension became transparent (approximately 1 h) and the liquid was then decanted and the nanoparticles washed with dry toluene. The combined toluene washings were concentrated in vacuo and the conversion determined by ^{1}H NMR spectroscopy. The residue was purified by column chromatography (hexane–CH$_2$Cl$_2$, 1 : 1) to give 14 as a white solid. Mp 62–64 °C; Enantiomeric excess was determined by CSP-HPLC: Chiralcel AD-H (4.6 mm × 25 cm), hexanes/i-PrOH, 90/10, 1 mL min^{-1}, RT, UV detection at 220 nm, retention times: 17 min (minor) and 29 min (major). $[\alpha]_D^{20}$ +4.6 (c 0.87, CHCl$_3$, 70% ee); δ_H (400 MHz, CDCl$_3$) 3.59 (s, 3H), 3.79 (s, 3H), 3.88 (d, J 9.0, 1H), 4.26 (app dt, 2H), 4.87–4.98 (m, 2H), 7.24–7.26 (m, 2H), 7.31–7.37 (m, 3H). The physical and spectroscopic

data associated with this compound are consistent with those in the literature.[36]

Siloxane 25

A 5 mL round bottom flask, equipped with a stirring bar, was charged with sulfonamide 4b (250 mg, 0.45 mmol) and azobi-sisobutyronitrile (AIBN, 38 mg, 0.23 mmol). The flask was fitted with a septum and flushed with argon. Dry toluene (2.0 mL) was added via syringe followed by 3-mercaptopropyltriethoxysilane (10, 270 µL, 1.13 mmol) and the resulting mixture was heated to 60 °C and stirred for 12 h. The solvent was removed in vacuo and the residue purified by column chromatography (EtOAc–NEt$_3$ 95 : 5) to give 25 in 65% yield (230 mg) as an amorphous white solid. Note: The ^{1}H-NMR spectrum of this compound indicates the presence of two rotameric species (rt, CDCl$_3$) in a 6/4 ratio. Mp 92–94 °C; $[\alpha]_D^{20}$ = +6.2 (c 0.75, CHCl$_3$); δ_H (600 MHz, CDCl$_3$) 0.66–0.80 (m, 2H), 0.88 (br dd, J 7.0, 13.1, 0.4H), 1.04 (br dd, J 7.0, 13.1, 0.6H), 1.19–1.28 (m, 9H), 1.36–1.52 (m, 3H), 1.53–1.84 (m, 6H), 2.38–2.59 (m, 4.6H), 2.73 (br d, J 12.9, 0.4H), 2.77–2.91 (m, 1H), 3.02–3.13 (m, 0.6H), 3.24–3.43 (m, 1.4H), 3.51 (br dd, J 18.1, 9.3, 1H), 3.78–3.86 (m, 6H), 3.95 (s, 1.8H), 4.04 (s, 1.2H), 4.60 (d, J 10.9, 0.6H), 4.82 (br s), 5.28 (d, J 10.9, 0.4H), 7.32–7.38 (m, 1.2H, 0.6H), 7.41–7.54 (m, 1.8H), 7.96 (d, J 9.0, 0.6H), 8.00 (d, J 9.0, 0.4H), 8.65 (d, J 4.2, 0.4H), 8.68 (d, J 4.2, 0.6H); v_{max}(neat)/cm^{-1} 2927, 1621, 1499, 1486, 1167, 1097, 1075, 985, 776, 715; m/z (ES) 792.2595 (M + H$^+$. C$_{35}$H$_{47}$N$_3$O$_6$F$_5$S$_2$Si requires 792.2596).

Magnetic nanoparticle-supported sulfonamide catalyst 24

A 5 mL round bottom flask was charged with 25 (0.020 mmol, 15.8 mg) and 2,5-diphenylfuran (internal standard, 0.020 mmol, 4.4 mg). The flask was placed under an argon atmosphere and fitted with a septum and dry CDCl$_3$ (0.5 mL) was added via syringe. The resulting solution was injected into a 20 mL reaction vessel previously charged with magnetite nanoparticles (200 mg) which had been suspended in dry CDCl$_3$ (0.5 mL) and sonicated for 5 min at room temperature and under argon. The resulting mixture was heated to 50 °C for 24 h under mechanical agitation. The vessel was then placed in proximity of an external magnet and the solution was separated from the nanoparticles via a Pasteur pipette. Catalyst loading (1.00 mmol g^{-1}) was determined by ^{1}H NMR spectroscopic analysis of the resulting solution which showed no traces of the peaks corresponding to the catalyst loading precursor. The remaining particles were subjected to five consecutive washing cycles with dry MTBE (methyl tert-butylether, 1.0 mL) before being evaluated as a recyclable catalyst.

General procedure for the evaluation of 24 in the desymmetrisation of meso anhydrides by methanolysis

A 10 mL reaction vessel was charged with the appropriate anhydride (0.2–0.4 mmol), fitted with a stirring bar and a septum and placed under an argon atmosphere. Dry MTBE (2.0–4.0 mL) and dry methanol (2.0–4.0 mmol) were injected via syringe and the mixture was stirred until all the anhydride had dissolved. The resulting solution was then transferred via syringe into the 20 mL vessel containing the supported catalyst 24 which had been previously suspended in dry MTBE (2.0–4.0 mL) and the final mixture was shaken (mechanical agitation) for the time indicated

in Tables 5–6, under an argon atmosphere. The vessel was then placed in proximity of an external magnet and the solution was separated from the nanoparticles *via* a Pasteur pipette. After 5 consecutive washing cycles with dry MTBE (1.0 mL), the combined organic washings were concentrated *in vacuo* and the crude product purified by column chromatography.

General procedure for the determination of the enantiomeric excess of hemiester products by derivatisation

A solution of thionyl chloride (9.0 µL, 0.12 mmol) in dry toluene (1 mL) was added to a solution of the appropriate monoester (0.10 mmol) in dry toluene (2 mL) at 0 °C and under an argon atmosphere. The mixture was stirred at 0 °C for 10 min. Dry NEt₃ (46.0 µL, 0.33 mmol) and (*R*)-1-(1-naphthyl)ethylamine, 18.0 µL 0.11 mmol) were added successively *via* syringe. The mixture was stirred at 0 °C for 1 h and at room temperature for an additional 1 h. The residue was then dissolved in ethyl acetate (15 mL). The organic solution was washed with HCl (1 N, 10 mL), saturated aq. NaHCO₃ (10 mL) and brine (10 mL). The organic layer was then dried over magnesium sulphate and concentrated *in vacuo* to give the diastereoisomeric mixture in quantitative yield. The enantiomeric excess of the appropriate hemiester could be determined by comparison of the product methyl ester resonances in the ¹H NMR spectrum and confirmed by CSP-HPLC analysis for some representative cases.

(1*S*,2*R*)-*cis*-2-Methoxycarbonylcyclohexane-1-carboxylic acid (22)

The described general methanolysis procedure (*vide supra*) was followed using *cis*-1,2-cyclohexanedicarboxylic anhydride (**19**, 61.7 mg, 0.40 mmol) and dry methanol (162 µL, 4.00 mmol) in MTBE (8.0 mL). After purification by flash chromatography, the desired monomethyl ester **22** was obtained in 97% yield (72.0 mg) as a colourless oil. The enantiomeric excess (78% *ee*) was determined by ¹H NMR spectroscopic analysis of the corresponding amide derived from (*R*)-1-(1-naphthyl)ethylamine, prepared as outlined above. $[\alpha]_D^{20} = +2.4$ (*c* 0.74 in CHCl₃), lit.[37] $[\alpha]_D^{25}$ −1.6 (*c* 4.4 in CHCl₃, 97% *ee*, (1*R*,2*S*)-enantiomer); δ_H (600 MHz, CDCl₃) 1.38–1.62 (m, 4H), 1.74–1.84 (m, 2H), 1.97–2.10 (m, 2H), 2.80–2.92 (m, 2H), 3.69 (s, 3H); δ_C (100 MHz, CDCl₃) 23.2, 23.3, 25.5, 25.8, 41.9, 42.1, 51.3, 173.7, 179.5. The NMR spectra data associated with this compound were consistent with those in the literature.[37]

(2*S*,3*R*)-*cis*-4-Methoxy-2,3-dimethyl-4-oxobutanoic acid (21)

The described general methanolysis procedure was followed using *meso*-2,3-dimethylsuccinic anhydride (**18**, 51.3 mg, 0.40 mmol) and dry methanol (162 µL, 4.00 mmol) in MTBE (8.0 mL). After purification by flash chromatography, the desired monomethyl ester **21** was obtained in 94% yield (60.2 mg) as a white solid. The enantiomeric excess (78% *ee*) was determined by ¹H NMR spectroscopic analysis of the corresponding amide derived from (*R*)-1-(1-naphthyl)ethylamine, prepared as outlined above. Mp 50–51 °C; (lit.,[38] 49 °C, rac); $[\alpha]_D^{20}$ −5.3 (*c* 1.16 in EtOH), lit.[37] $[\alpha]_D^{25}$ +8.4 (*c* 1.40, EtOH, 98% *ee*, (2*R*,3*S*)-enantiomer); δ_H (400 MHz, CDCl₃) 1.20–1.30 (m, 6H), 2.76–2.90 (m, 2H), 3.73 (s, 3H); δ_C (100 MHz, CDCl₃) 14.6, 14.8, 42.1, 42.3, 51.9, 175.0, 180.2.

(2*S*,3*R*)-3-*endo*-Methoxycarbonylbicyclo[2.2.1]hept-5-ene-2-*endo*-carboxylic acid (28)

The described general methanolysis procedure was followed using *cis*-5-norbornene-*endo*-2,3-dicarboxylic anhydride (**26**, 32.8 mg, 0.20 mmol) and dry methanol (81.0 µL, 2.00 mmol) in MTBE (4.0 mL). After purification by flash chromatography, the desired monomethyl ester **28** was obtained in 92% yield (36.1 mg) as a white solid. The enantiomeric excess (82% *ee*) was determined by ¹H NMR spectroscopic analysis of the corresponding amide derived from (*R*)-1-(1-naphthyl)ethylamine, prepared as outlined above. This could be confirmed by CSP-analysis of the amide derivative: Chiralpak AD-H (4.6 mm × 25 cm), hexane–IPA: 90/10, 0.75 mL min⁻¹, RT, UV detection at 220 nm, retention times: 11.0 min (major diastereomer) and 16.5 (minor diastereomer). Mp 75–76 °C; (lit.,[39] 75–78 °C). $[\alpha]_D^{20}$ −7.4 (*c* 1.53, CCl₄); lit.[39] $[\alpha]_D^{rt}$ = −7.8 (*c* 4.76, CCl₄, 99% *ee*); δ_H (600 MHz, CDCl₃) 1.36 (app. br d, 1H), 1.52 (app. dt, 1H), 3.15–3.28 (m, 2H), 3.31 (dd, J 10.0, 3.0, 1H), 3.37 (dd, J 10.0, 3.0, 1H), 3.62 (s, 3H), 6.24 (dd, J 5.5, 3.0, 1H), 6.36 (dd, J 5.5, 3.0, 1H); δ_C (150 MHz, CDCl₃) 46.1, 46.6, 48.0, 48.2, 48.8, 51.5, 134.3, 135.6, 172.9, 178.2.

(2*S*,3*R*)-3-*exo*-Methoxycarbonylbicyclo[2.2.1]hept-5-ene-2-*exo*-carboxylic acid (29)

The described general methanolysis procedure was followed using *cis*-5-norbornene *exo*-2,3-dicarboxylic anhydride (**27**, 32.8 mg, 0.20 mmol) and dry methanol (81.0 µL, 2.00 mmol) in MTBE (4.0 mL). After purification by flash chromatography, the desired monomethyl ester **29** was obtained in 97% yield (38.0 mg) and as a as a white solid. The enantiomeric excess (79% *ee*) was determined by ¹H NMR spectroscopic analysis of the corresponding amide derived from (*R*)-1-(1-naphthyl)ethylamine, prepared as outlined above. Mp 61–62 °C; (lit.,[39] 61 °C); δ_H (600 MHz, CDCl₃) 1.53 (app. dt, 1H), 2.12 (app. br d, 1H), 2.67–2.69 (m, 2H), 3.13–3.17 (m, 2H), 3.68 (s, 3H), 6.23–6.27 (m, 2H); δ_C (100 MHz, CDCl₃) 44.9, 45.0, 45.3, 46.8, 47.0, 51.4, 137.4, 137.6, 173.4, 178.8.

(1*S*,2*R*)-6-(Allyloxycarbonyl)cyclohex-3-enecarboxylic acid (30, cycle 29)

A 10 mL reaction vessel was charged with *cis*-1,2,3,6-tetrahydrophthalic anhydride (**20**, 30.4 mg, 0.20 mmol), fitted with a septum and placed under an argon atmosphere. Anhydrous MTBE (2.0 mL) and dry allyl alcohol (137 µL, 2.00 mmol) were injected *via* syringe and the mixture was stirred until all the anhydride had dissolved. The resulting solution was then transferred *via* syringe into the 20 mL vessel containing the MNP-supported catalyst which had been previously suspended in dry MTBE (2.0 mL) and the final mixture was shaken (mechanical agitation) for 48 h at room temperature and under an argon atmosphere. The vessel was then placed in proximity of an external magnet and the solution was separated from the nanoparticles *via* a Pasteur pipette. After 5 consecutive washing cycles with dry MTBE (1.0 mL), the combined organic washings were concentrated *in vacuo* and the crude product purified by column chromatography to obtain the desired monoallyl ester **30** in 83% yield (35.0 mg) as a colourless oil. The enantiomeric excess (82% *ee*) was determined by ¹H NMR spectroscopic analysis of the corresponding amide derived from (*R*)-1-(1-naphthyl)ethylamine,

prepared as outlined above. This could be confirmed by CSP-analysis of the amide derivative: Chiralcel OD-H (4.6 mm × 25 cm), hexane–IPA: 95 : 5, 1.0 mL min⁻¹, RT, UV detection at 220 nm, retention times: 17.0 min (minor diastereomer) and 20.0 (major diastereomer). δ_H (400 MHz, CDCl₃) 2.34–2.48 (m, 2H, H-3b and H-6b), 3.55–2.69 (m, 2H), 3.06–3.16 (m, 2H), 4.57–4.68 (m, 2H), 5.24 (dd, 1H, *J* 10.5, 1.5), 5.33 (dd, 1H, *J* 17.1, 1.5), 5.66–5.77 (m, 2H), 5.86–5.97 (m, 1H); δ_C (125 MHz, CDCl₃) 25.1, 25.3, 39.0, 39.1, 65.0, 117.7, 124.6, 124.7, 131.5, 172.4, 178.4; ν_{max}(neat)/cm⁻¹ 3029, 2924, 1730, 1701, 1183, 1158, 933, 659; *m/z* (ES) 209.0809 (M − H⁺. C₁₁H₁₃O₄ requires 209.0814).

(1*S*,2*R*)-*cis*-2-Methoxycarbonylcyclohex-4-ene-1-carboxylic acid (23, cycle 30)

The described general methanolysis procedure was followed using *cis*-1,2,3,6-tetrahydrophthalic anhydride (**20**, 60.9 mg. 0.40 mmol) and dry methanol (162 μL, 4.00 mmol) in MTBE (8.0 mL). After purification by flash chromatography, the desired monomethyl ester **23** was obtained in 92% yield (67.8 mg) as a colourless oil. The enantiomeric excess (78% *ee*) was determined by ¹H NMR spectroscopic analysis of the corresponding amide derived from (*R*)-1-(1-naphthyl)ethylamine, prepared as outlined above. This could be confirmed by CSP-analysis of the amide derivative: Chiralcel OD-H (4.6 mm × 25 cm), hexane–IPA: 93 : 7, 0.50 mL min⁻¹, RT, UV detection at 220 nm, retention times: 34.4 min (minor diastereomer) and 40.4 (major diastereomer). $[\alpha]_D^{20}$ −1.6 (*c* 1.22 in CHCl₃), lit.⁴⁰ $[\alpha]_D^{25}$ −3.44 (*c* 1.68, CHCl₃, 99% *ee*); δ_H (400 MHz, CDCl₃) 2.34–2.45 (m, 2H), 2.55–2.65 (m, 2H), 3.05–3.13 (m, 2H), 3.72 (s, 3H), 5.70 (m, 2H); δ_C (100 MHz, CDCl₃) 25.1, 25.3, 39.0, 39.1, 51.5, 124.6, 124.7, 173.2, 179.0.

Notes and references

1 For selected recent reviews see: (*a*) T. E. Kristensen and T. Hansen, *Eur. J. Org. Chem.*, 2010, **17**, 3179; (*b*) M. Bengalia, A. Puglisi and F. Cozzi, *Chem. Rev.*, 2003, **103**, 3401; (*c*) C. E. Song, *Annu. Rep. Prog. Chem., Sect. C*, 2005, **101**, 143; (*d*) F. Cozzi, *Adv. Synth. Catal.*, 2006, **348**, 1367; (*e*) M. Bengalia, *New J. Chem.*, 2006, **30**, 1525; (*f*) A. Corma and H. Garcia, *Adv. Synth. Catal.*, 2006, **348**, 1391; (*g*) M. Gruttadauria, F. Giacalone and R. Noto, *Chem. Soc. Rev.*, 2008, **37**, 1666.

2 Very recently Zipse have tackled this reactivity problem in the context of polymer-bound DMAP-based organocatalysts by immobilising highly active tricyclic 3,4-diaminopyridines (which are considerably more active than DMAP itself) on a polymer support. The resulting polymers were comparable in terms of activity with homogeneous DMAP. See: V. D'Elia, Y. Liu and H. Zipse, *Eur. J. Org. Chem.*, 2011, 1527.

3 (*a*) For a recent review of the emerging field of magnetic nanoparticle synthesis and application see:A.-H. Lu, E. L. Salabas and F. Schüth, *Angew. Chem., Int. Ed.*, 2007, **46**, 1222see also; (*b*) G. A. Somorjai and J. Y. Park, *Angew. Chem., Int. Ed.*, 2008, **47**, 9212.

4 Recent reviews: (*a*) Y. H. Zhu, L. P. Stubbs, F. Ho, R. Z. Liu, C. P. Ship, J. A. Maguire and N. S. Hosmane, *ChemCatChem*, 2010, **2**, 365; (*b*) V. Polshettiwar and R. S. Varma, *Green Chem.*, 2010, **12**, 743; (*c*) A. Schätz, O. Reiser and W. J. Stark, *Chem.–Eur. J.*, 2010, **16**, 8950; (*d*) C. W. Lim and I. S. Lee, *Nano Today*, 2010, **5**, 412; (*e*) S. Shylesh, V. Schünemann and W. R. Thiel, *Angew. Chem., Int. Ed.*, 2010, **49**, 3428; (*f*) K. V. S. Ranganath and F. Glorius, *Catal. Sci. Technol.*, 2011, **1**, 13.

5 (*a*) H. M. R. Gardimalla, D. Mandal, P. D. Stevens, M. Yen and Y. Gao, *Chem. Commun.*, 2005, 4432; (*b*) M. Kawamura and K. Sato, *Chem. Commun.*, 2006, 4718; (*c*) N. T. S. Phan, C. S. Gill, J. V. Nguyen, Z. J. Zhang and C. W. Jones, *Angew. Chem., Int. Ed.*, 2006, **45**, 2209; (*d*) N. T. S. Phan and C. W. Jones, *J. Mol. Catal. A: Chem.*, 2006, **253**, 123; (*e*) M. Kawamura and K. Sato, *Chem. Commun.*, 2007, 3404; (*f*) C. S. Gill, B. A. Pryce and C. W. Jones, *J. Catal.*, 2007, **251**, 145; (*g*) S. Luo,

X. Zheng, H. Xu, X. Mi, L. Zhang and J.-P. Cheng, *Adv. Synth. Catal.*, 2007, **349**, 243; (*h*) S. Luo, X. Zheng and J.-P. Cheng, *Chem. Commun.*, 2008, 5719; (*i*) A. Schätz, R. N. Grass, W. J. Stark and O. Reiser, *Chem.–Eur. J.*, 2008, **14**, 8262; (*j*) V. Polshettiwar, B. Baruwati and R. S. Varma, *Chem. Commun.*, 2009, 1837; (*k*) Y. Zhang, Y. Zhao and C. Xia, *J. Mol. Catal. A: Chem.*, 2009, **306**, 107; (*l*) V. Polshettiwar and R. S. Varma, *Tetrahedron*, 2010, **66**, 1091; (*m*) P. Riente, C. Mendoza and M. A. Pericás, *J. Mater. Chem.*, 2011, **21**, 7350.

6 (*a*) L. M. Litvinenko and A. I. Kirichenko, *Dokl. Chem.*, 1967, 763; (*b*) W. Steglich and G. Höfle, *Angew. Chem., Int. Ed. Engl.*, 1969, **8**, 981.

7 J. E. Murtagh, S. H. McCooey and S. J. Connon, *Chem. Commun.*, 2005, 227.

8 C. Ó Dalaigh, S. A. Corr, Y. Gun'ko and S. J. Connon, *Angew. Chem., Int. Ed.*, 2007, **46**, 4329.

9 Recent reviews concerning chiral DMAP-derivatives: (*a*) C. E. Müller and P. R. Schreiner, *Angew. Chem., Int. Ed.*, 2011, **50**, 6012; (*b*) A. C. Spivey, P. McDaid, in *Enantioselective Organocatalysis*, (Ed: P. Dalko), Wiley-VCH Verlag, Weinheim, 2007, pp. 287–329; (*c*) R. P. Wurz, *Chem. Rev.*, 2007, **107**, 5570; (*d*) S. J. Connon, *Lett. Org. Chem.*, 2006, **3**, 333; (*e*) E. R. Jarvo and S. J. Miller, in *Comprehensive Asymmetric Catalysis*, Supplement 1; (eds: E. N. Jacobsen, A. Pfaltz, H. Yamamoto), Springer-Verlag, Berlin, Heidelberg, 2004; Chapter 43; (*f*) S. J. Miller, *Acc. Chem. Res.*, 2004, **37**, 601; (*g*) G. C. Fu, *Acc. Chem. Res.*, 2004, **37**, 542.

10 Selected leading references concerning the design and application of chiral DMAP (and related systems) analogues: (*a*) E. Vedejs and X. Chen, *J. Am. Chem. Soc.*, 1996, **118**, 1809; (*b*) E. Vedejs, O. Daugulis and S. T. Diver, *J. Org. Chem.*, 1996, **61**, 430; (*c*) E. Vedejs and O. Daugulis, *J. Am. Chem. Soc.*, 2003, **125**, 4166; (*d*) J. C. Ruble and G. C. Fu, *J. Org. Chem.*, 1996, **61**, 7230; (*e*) C. E. Garrett, M. M.-C. Lo and G. C. Fu, *J. Am. Chem. Soc.*, 1998, **120**, 7479; (*f*) T. Kawabata, M. Nagato, K. Takasu and K. Fuji, *J. Am. Chem. Soc.*, 1997, **119**, 3169; (*g*) T. Kawabata, Y. Yamamoto, H. Yoshida, Y. Nagaoka and K. Fuji, *Chem. Commun.*, 2001, 2700; (*h*) A. C. Spivey, T. Fekner and H. Adams, *Tetrahedron Lett.*, 1998, **39**, 8919; (*i*) A. C. Spivey, D. P. Leese, F. Zhu, S. G. Davey and R. L. Jarvest, *Tetrahedron*, 2004, **60**, 4513; (*j*) T. Oriyama, K. Imai, T. Sano and T. Hosoya, *Tetrahedron Lett.*, 1998, **39**, 3529; (*k*) S. J. Miller, G. T. Copeland, N. Papaioannou, T. E. Horstmann and E. M. Ruel, *J. Am. Chem. Soc.*, 1998, **120**, 1629; (*l*) G. T. Copeland and S. J. Miller, *J. Am. Chem. Soc.*, 2001, **123**, 6496; (*m*) G. Priem, B. Pelotier, S. J. F. Macdonald, M. S. Anson and I. B. Campbell, *J. Org. Chem.*, 2003, **68**, 3844; (*n*) K. Ishihara, Y. Kosugi and M. Akahura, *J. Am. Chem. Soc.*, 2004, **126**, 12212; (*o*) Y. Suzuki, K. Yamauchi, K. Muramatsu and M. Sato, *Chem. Commun.*, 2004, 2770; (*p*) T. Kano, K. Sasaki and K. Maruoka, *Org. Lett.*, 2005, **7**, 1347; (*q*) G. T. Notte, T. Sammakia and P. J. Steel, *J. Am. Chem. Soc.*, 2005, **127**, 13502; (*r*) S. Yamada, T. Misono and Y. Iwai, *Tetrahedron Lett.*, 2005, **46**, 2239; (*s*) V. B. Birman, E. W. Uffman, H. Jiang, X. Li and C. J. Kilbane, *J. Am. Chem. Soc.*, 2004, **126**, 12227; (*t*) V. B. Birman and H. Jiang, *Org. Lett.*, 2005, **7**, 2445; (*u*) T. Poisson, M. Penhoat, G. Dupas, C. Papamicaël, V. Dalla and F. Marsais, *Synlett*, 2005, 2285; (*v*) H. V. Nguyen, D. C. D. Butler and C. J. Richards, *Org. Lett.*, 2006, **8**, 769; (*w*) S. Yamada, T. Misono, Y. Iwai, A. Masumizu and Y. Akiyama, *J. Org. Chem.*, 2006, **71**, 6872; (*x*) C. Kanta De, E. G. Klauber and D. Seidel, *J. Am. Chem. Soc.*, 2009, **131**, 17060; (*y*) E. G. Klauber, C. Kanta De, T. K. Shah and Daniel Seidel, *J. Am. Chem. Soc.*, 2010, **132**, 13624; (*z*) E. G. Klauber, N. Mittal, T. K. Shah and Daniel Seidel, *Org. Lett.*, 2011, **13**, 2464.

11 (*a*) C. Ó Dálaigh, S. J. Hynes, D. J. Maher and S. J. Connon, *Org. Biomol. Chem.*, 2005, **3**, 981; (*b*) C. Ó Dálaigh, S. J. Hynes, J. E. O'Brien, T. McCabe, D. J. Maher, G. W. Watson and S. J. Connon, *Org. Biomol. Chem.*, 2006, **4**, 2785; (*c*) C. Ó Dálaigh and S. J. Connon, *J. Org. Chem.*, 2007, **72**, 7066.

12 M. Alvarez-Pérez, S. M. Goldup, D. A. Leigh and A. M. Z. Slawin, *J. Am. Chem. Soc.*, 2008, **130**, 1836.

13 Selected relevant reviews: (*a*) M. S. Taylor and E. N. Jacobsen, *Angew. Chem., Int. Ed.*, 2006, **45**, 1520; (*b*) S. J. Connon, *Chem.–Eur. J.*, 2006, **12**, 5418; (*c*) S. J. Connon, *Chem. Commun.*, 2008, 2499; (*d*) S. J. Connon, *Synlett.*, 2009, 354; (*e*) X. Yu and W. Wang, *Chem.–Asian J.*, 2008, **3**, 516; (*f*) H. Hiemstra and T. Marcelli, *Synthesis*, 2010, 1229.

14 (*a*) S. H. McCooey and S. J. Connon, *Angew. Chem., Int. Ed.*, 2005, **44**, 6367; (*b*) S. H. McCooey, T. McCabe and S. J. Connon, *J. Org. Chem.*, 2006, **71**, 7494.

15 A. Peschiulli, C. Quigley, S. Tallon, Y. K. Gun'ko and S. J. Connon, *J. Org. Chem.*, 2008, **73**, 6409.

16 A. Peschiulli, Y. Gun'ko and S. J. Connon, *J. Org. Chem.*, 2008, **73**, 2454.

17 C. Palacio and S. J. Connon, *Org. Lett.*, 2011, **13**, 1298.

18 S. Tallon, A. C. Lawlor and S. J. Connon, *Arkivoc*, 2011, **iv**, 115.

19 Selected examples: (*a*) B.-J. Li, L. Jiang, M. Liu, Y.-C. Chen, L.-S. Ding and Y. Wu, *Synlett*, 2005, 603; (*b*) B. Vakulya, S. Varga, A. Csámpai and T. Soós, *Org. Lett.*, 2005, **7**, 1967; (*c*) J. Ye, D. J. Dixon and P. S. Hynes, *Chem. Commun.*, 2005, 4481; (*d*) A. E. Mattson, A. M. Zuhl, T. E. Reynolds and K. A. Scheidt, *J. Am. Chem. Soc.*, 2006, **128**, 4932; (*e*) G. Bartoli, M. Bosco, A. Carlone, M. Locatelli, A. Mazzanti, L. Sambri and P. Melchiorre, *Chem. Commun.*, 2007, 722; (*f*) P. S. Hynes, D. Stranges, P. A. Stupple, A. Guarna and D. J. Dixon, *Org. Lett.*, 2007, **9**, 2107; (*g*) T.-Y. Liu, H.-L. Cui, Q. Chai, J. Long, B.-J. Li, Y. Wu, L.-S. Ding and Y.-C. Chen, *Chem. Commun.*, 2007, 2228; (*h*) J. Lubkoll and H. Wennemers, *Angew. Chem., Int. Ed.*, 2007, **46**, 6841; (*i*) P. Dinér, M. Nielsen, S. Bertelsen, B. Niess and K. A. Jørgensen, *Chem. Commun.*, 2007, 3646; (*j*) H. Li, L. Zu, J. Wang and W. Wang, *Tetrahedron Lett.*, 2006, **47**, 3145; (*k*) T.-Y. Liu, R. Li, Q. Chai, J. Long, B.-J. Li, Y. Wu, L.-S. Ding and Y.-C. Chen, *Chem.–Eur. J.*, 2007, **13**, 319; (*l*) J. Wang, H. Li, L. Zu, W. Jiang, H. Xe, W. Duan and W. Wang, *J. Am. Chem. Soc.*, 2006, **128**, 12652; (*m*) C.-L. Gu, L. Liu, Y. Sui, J.-L. Zhao, D. Wang and Y.-J. Chen, *Tetrahedron: Asymmetry*, 2007, **18**, 455; (*n*) M. M. Biddle, M. Lin and K. A. Scheidt, *J. Am. Chem. Soc.*, 2007, **129**, 3830; (*o*) J. Wang, L. Zu, H. Li, H. Xe and W. Wang, *Synthesis*, 2007, 2576; (*p*) L. Zu, J. Wang, H. Li, H. Xe, W. Jiang and W. Wang, *J. Am. Chem. Soc.*, 2007, **129**, 1036; (*q*) B. Wang, F. Wu, Y. Wang, X. Liu and L. Deng, *J. Am. Chem. Soc.*, 2007, **129**, 768; (*r*) L. Bernardi, F. Fini, R. P. Herrera, A. Ricci and V. Sgarzani, *Tetrahedron*, 2006, **62**, 375; (*s*) C. M. Bode, A. Ting and S. E. Schaus, *Tetrahedron*, 2006, **62**, 11499; (*t*) A. L. Tillman, J. Ye and D. J. Dixon, *Chem. Commun.*, 2006, 1191; (*u*) J. Song, W. Wang and L. Deng, *J. Am. Chem. Soc.*, 2006, **128**, 6048; (*v*) J. Song, H.-W. Shih and L. Deng, *Org. Lett.*, 2007, **9**, 603; (*w*) Y.-Q. Wang, J. Song, R. Hong, H. Li and L. Deng, *J. Am. Chem. Soc.*, 2006, **128**, 8156; (*x*) Y. Wang, H. Li, Y.-Q. Wang, Y. Liu, B. M. Foxman and L. Deng, *J. Am. Chem. Soc.*, 2007, **129**, 6364; (*y*) M. Amere, M.-C. Lasne and J. Rouden, *Org. Lett.*, 2007, **9**, 2621; (*z*) Y. Wang, R.-G. Han, Y.-L. Zhao, S. Yang, P.-F. Xu and D. J. Dixon, *Angew. Chem., Int. Ed.*, 2009, **48**, 9834.

20 For the first example of the use of C-9 substituted sulfonamide-based cinchona alkaloid-based catalysts see ref. 19c.

21 (*a*) S. H. Oh, H. S. Rho, J. W. Lee, J. E. Lee, S. H. Youk, J. Chin and C. E. Song, *Angew. Chem., Int. Ed.*, 2008, **47**, 7872; (*b*) S. E. Park, E. H. Nam, H. B. Jang, J. S. Oh, S. Some, Y. S. Lee and C. E. Song, *Adv. Synth. Catal.*, 2010, **352**, 2211.

22 A. Peschiulli, B. Procuranti, C. J. O'Connor and S. J. Connon, *Nat. Chem.*, 2010, **2**, 380.

23 Preliminary communication: O. Gleeson, R. Tekoriute, Y. K. Gun'ko and S. J. Connon, *Chem.–Eur. J.*, 2009, **15**, 5669.

24 See the Experimental section and supplementary information for details.† These nanoparticles have been characterized by FTIR and Raman spectroscopy, XRD patterns, and TEM analysis.

25 (*a*) R. Massart, *IEEE Trans. Magn.*, 1981, **17**, 1247; (*b*) X. P. Qiu, *Chin. J. Chem.*, 2000, **18**, 834.

26 B. Pelotier, G. Priem, I. B. Campbell, S. J. F. Macdonald and M. S. Anson, *Synlett*, 2003, 679.

27 (*a*) P. Yu, J. He and C. Guo, *Chem. Commun.*, 2008, 2355see also: (*b*) P. Yu, J. He, Lan Yang, Min Pu and X. Guo, *J. Catal.*, 2008, **260**, 81.

28 For a recent example of the immobilisation of monofunctional (thio)urea catalysts on silica see:H.-T. Chen, B. G. Trewyn, J. W. Wiench, M. Pruski and V. S.-Y. Lin, *Top. Catal.*, 2010, **53**, 187.

29 H. Miyabe, S. Tuchida, M. Yamauchi and Y. Takemoto, *Synthesis*, 2006, 3295.

30 For examples of the use of this radical-initiated strategy to immobilise cinchona alkaloids see: (*a*) P. Hodge, E. Khoshdel and J. Waterhouse, *J. Chem. Soc., Perkin Trans. 1*, 1985, 2327; (*b*) H. S. Kim, Y. M. Song, J. S. Choi, J. W. Yang and H. Han, *Tetrahedron*, 2004, **60**, 12051.

31 It is noteworthy that at 2 mol% loading the enantiomeric excess of the product improved to 88%. The considerably lower activity of the heterogeneous catalyst **21** precluded its effective use at this lower loading.

32 S. H. Youk, S. H. Oh, H. S. Rho, J. E. Lee, J. W. Lee and C. E. Song, *Chem. Commun.*, 2009, 2220.

33 (*a*) F. Bigi, S. Carloni, R. Maggi, A. Mazzacani, G. Sartori and G. Tanzi, *J. Mol. Catal. A: Chem.*, 2002, **182**, 533; (*b*) Y. M. Song, J. S. Choi, J. W. Yang and H. Han, *Tetrahedron Lett.*, 2004, **45**, 3301; (*c*) H. S. Kim, Y. M. Song, J. S. Choi, J. W. Yang and H. Han, *Tetrahedron*, 2004, **60**, 12051.

34 Selected reviews: (*a*) A. C. Spivey and B. I. Andrews, *Angew. Chem., Int. Ed.*, 2001, **40**, 3131; (*b*) Y. Chen, P. McDaid and L. Deng, *Chem. Rev.*, 2003, **103**, 2965; (*c*) I. Atodiresei, I. Schiffers and C. Bolm, *Chem. Rev.*, 2007, **107**, 5683.

35 For a very recent report detailing an organocatalyst that can be recycled 30 times see: Y. Arakawa, M. Wiesner and H. Wennemers, *Adv. Synth. Catal.*, 2011, **353**, 1201.

36 M. Terada, H. Ube and Y. Yaguchi, *J. Am. Chem. Soc.*, 2006, **128**, 1454.

37 Y. Chen, S. K. Tian and L. Deng, *J. Am. Chem. Soc.*, 2000, **122**, 9542.

38 W. A. Bone, J. J. Sudborough and C. H. G. Sprankling, *J. Chem. Soc. Trans.*, 1904, **85**, 539.

39 C. Bolm, I. Schiffers, C. L. Dinter and A. Gerlach, *J. Org. Chem.*, 2000, **65**, 6984.

40 N. Tamura, Y. Kawano, Y. Matsushita, K. Yoshioka and M. Ochiai, *Tetrahedron Lett.*, 1986, **27**, 3749.